

Note: This is a draft of a paper submitted for publication. Contents of this paper should not be quoted or referred to without permission of the author(s).

Nanoparticle Arrays of Ni, Fe, Co, CoPt, and FePt: Ion Beam Synthesis and Competing Magnetic Energy Scales

J. R. Thompson^{a,b}, K.D. Sorge^{a,b}, L.A. Boatner^a, J.D. Budai^a, T.E. Haynes^a, Hwee Kwan Lee^a, A. Meldrum^c, T.C. Schulthess^a, C.W. White^a, S.P. Withrow^a, and A. Meldrum^c

^aOak Ridge National Laboratory, Oak Ridge, TN 37831

^bUniversity of Tennessee, Knoxville, Tennessee

^cUniversity of Alberta, Edmonton, Alberta, Canada

Proceedings for the
2003 NANOMAT International Congress on Materials Science and Nanotechnologies
European Academy of Sciences
Brussels, Belgium
October 22–24, 2003

"The submitted manuscript has been authored by a contractor of the U.S. Government under contract No. DE-AC05-00OR22725. Accordingly, the U.S. Government retains a nonexclusive, royalty-free license to publish or reproduce the published form of this contribution, or allow others to do so, for U.S. Government purposes."

prepared by
CONDENSED MATTER SCIENCES DIVISION
OAK RIDGE NATIONAL LABORATORY

Managed by
UT- BATTTELLE, LLC

under
Contract No. DE-AC05-00OR22725
with the
U.S. DEPARTMENT OF ENERGY
Oak Ridge, Tennessee

March. 04

Nano-particle arrays of Ni, Fe, Co, CoPt, and FePt: ion beam synthesis and competing magnetic energy scales

James R. Thompson and Korey D. Sorge

*Dept. of Physics, University of Tennessee, Knoxville, Tennessee 37996 USA
and Condensed Matter Sciences Division, Oak Ridge National Lab, Oak Ridge, Tennessee
37831 USA*

**Lynn A. Boatner, John D. Budai, Tony E. Haynes, Hwee Kwan Lee, Thomas C. Schulthess,
C. W. White, and Steven P. Withrow**

*Condensed Matter Sciences Division, Oak Ridge National Lab, Oak Ridge, Tennessee 37831
USA*

Alkiviathes Meldrum

*Department of Physics,
University of Alberta, Edmonton, Alberta, Canada*

(Submitted for the Proceedings of the 2003 NANOMAT International Congress on Materials Science and Nanotechnologies, sponsored by the European Academy of Sciences (Brussels, 22-24 October 2003) (invited presentation).

SUMMARY

We have investigated the synthesis and magnetic properties of a series of nanoparticle systems containing Ni, Fe, Co, CoPt, or FePt. A dispersed array of nanoparticles was formed by implanting ions of the elements into either single crystal hosts such as Al₂O₃ and yttrium-stabilized cubic zirconia (YSZ) or amorphous SiO₂, to fluences of $\sim 10^{17}$ ions/cm². Subsequent heat treatment precipitated metallic particles from the supersaturated solution, forming a buried layer of dispersed, electrically isolated particles with a peak concentration of ~ 10 % by volume. X-ray diffraction and transmission electron microscopy studies showed that the particles are often faceted and preferentially textured by a crystalline matrix, with typical particle dimensions of a few nm. For the FePt intermetallic, XRD showed considerable ordering into the high anisotropy L1₀ phase after annealing in a reducing atmosphere, while the ordering in CoPt was more limited.

Magnetic studies of these systems revealed a competition between at least four energy scales: the usual “Zeeman” interaction between a magnetic moment and an external field, magnetocrystalline anisotropy, a magnetostatic inter-particle interaction, and the thermal energy. We have explored this competition by investigations of the magnetic response as a function of magnetic field H , temperature T , and orientation, for ferromagnetic materials (Ni, Fe, ..., FePt) in which the bulk magnetocrystalline anisotropy varies by several orders-of-magnitude. For example, α -Fe nanoparticles in YSZ are dominated by magnetostatic interactions, which make the in-plane direction the easy axis and serve to stabilize the remanence to temperatures far above the expected “blocking” temperature where the magnetic ‘memory’ would be lost. The essential role of inter-particle interactions in stabilizing the remanent magnetization has been demonstrated by numerical simulations, using the observed distributions and sizes of the particles. In contrast, ordered FePt nanoparticles are governed primarily by strong magnetocrystalline anisotropy up to temperatures near their measured Curie points, $T_c \approx 700$ -730 K. These and related examples illustrate some of the rich diversity of magnetic phenomena in nanoparticle systems.

INTRODUCTION

The study of magnetic structures with relevant length scales of a few nanometers is an exciting branch of condensed matter physics. Not only do these structures behave very differently than their bulk counterparts due to an enhanced surface-to-volume ratio [Bi1994], but we are able to limit and control a variety of different magnetic phenomena. They offer particularly rich and attractive systems for magnetic investigations and provide useful models for exploring the competition of various energies that can affect very important technologies. A central example is the phenomenon of “superparamagnetism” (where thermal disorder “erases” information stored on magnetic media), which threatens to cut off the exponentially growing storage density in hard disk drives. [We1999]

A useful introduction to many aspects of magnetic nanostructured materials has been given by Leslie-Pelecky and Rieke. [Le1996] Some specific phenomena (spin ordering, thermal excitations, relaxation of magnetization) in non-interacting nanoparticles are discussed in the

reviews of Kodama [Ko1999] and Skomski. [Sk2003] For cases where interactions play an important role, see Hanson and Mørup [Ha1998] for a review of models for relaxation of the magnetization.

Block copolymer fabrication [Su2000], [Ha2001] of magnetic nanoparticles is a popular method of making particles of controlled composition and self-assembling them on a surface. This technique provides great control of the particle separation and size distribution, but is not able to crystallographically texture particles or give a varying depth profile. Cluster depositing particles [Xu2003] gives greater control of the depth profile and size distribution, but still offers no crystallographic texturing. The objectives of the present report are to describe a versatile (but less familiar) ion-beam-based method for synthesis of nanoparticle systems that does offer the possibility of controlling particle orientation, and then to illustrate and discuss qualitatively some magnetic phenomena in the materials, from the perspective of competing energy scales.

ION BEAM SYNTHESIS of MATERIALS

Ion implantation provides a means for incorporating a foreign element or elements into a host material by use of an energetic beam of ions of the element(s). [Pi1985] It is a powerful tool for tailoring the properties of materials near their surface, independent of the bulk properties. The technique became popular with physicists and nuclear chemists in the 1960's, but the technology most impacted by ion beam technology was the microelectronics industry, where ion implantation has been used to reproducibly dope Si for electronic devices. In general, many different ion species can be implanted into a wide variety of hosts, thereby providing a versatile research and development tool.

In practice, energetic ions from an accelerator form a layer of implanted material in the host (substrate) material, where collisions with electrons and nuclei in the target bring the ion to rest. The projected range and range spread depend on the implant energy, mass of the ion, and atomic mass of the host. Typical ranges are 10 nm – 1 μm ; the concentration profile is approximately Gaussian, although multiple implantation steps can alter the distribution with depth. Additional advantages of ion implantation are its reproducibility and the control over how many ions are introduced, as determined by the integrated ion current. A disadvantage is damage to the target, since collisions with atoms in the lattice can displace them to interstitial sites and form vacancies. In severe cases, the substrate can be amorphized in the near-surface implanted region, with attendant adverse effects on the electronic and magnetic properties. Processing at elevated temperatures, e.g., during the implantation, promotes diffusion and can reduce initial damage and minimize amorphization.

To form nanoparticles of binary magnetic alloys and intermetallic compounds, ions of two different elements were sequentially implanted to have overlapping concentration profiles. For example, to form $\text{Fe}_{1-x}\text{Pt}_x$ in sapphire, single crystal substrates of *c*-axis-oriented Al_2O_3 were implanted first with Fe (350 keV) and then with Pt (910 keV) to give overlapping implant profiles of Fe and Pt, each with a projected range of ~ 175 nm. The ion doses were controlled to obtain a desired composition; e.g. for an alloy with a Pt atomic fraction of 45% [= Pt dose/(Fe dose + Pt dose)] where the magnetic coercivity is near maximum, doses of $1 \times 10^{17}/\text{cm}^2$ for Fe

and $8.2 \times 10^{16}/\text{cm}^2$ for Pt were used. The ion implantation was carried out at elevated temperatures (550°C for Fe and 500°C for Pt) in order to prevent the near surface of the Al_2O_3 substrate from being rendered amorphous by implantation-induced displacive radiation damage.

In most cases of interest here, the implanted species are immiscible in the host and form a supersaturated solution of nominally isolated dopants with concentrations typically

up to ~10-15 at %. Upon thermal annealing (generally in forming gas Ar + 4 at% H_2), diffusion causes most of the implanted material to precipitate as nano-particles. This also improves the crystallinity of the matrix. For the above example of $\text{Fe}_{1-x}\text{Pt}_x$ in sapphire, the samples were annealed at 1100°C for 2 hours. The formation of particles below the surface of the host protects the nanoparticles from corrosion and damage; furthermore, the use of insulating hosts [sapphire (Al_2O_3), YSZ (yttria-stabilized zirconia), quartz (SiO_2), etc.] eliminates direct electron exchange between particles, thereby removing this form of inter-particle magnetic interaction. Table I lists some of the systems of magnetic nanoparticles and host matrices that have been investigated.

A variety of particle morphologies are obtained, as observed by transmission electron microscopy. For non-crystalline hosts such as quartz, the particles tend to be spherical or nearly so, and randomly oriented crystallographically. In crystalline hosts, however, the particles often exhibit preferred alignments, as for Ni or Fe in sapphire, Fe in YSZ, etc., and they are faceted in many cases. For other materials, e.g., FePt implanted into sapphire at comparatively low temperatures, larger planar structures together with more isolated particles have been observed. Diameters of isolated particles are typically in the range of 1 – 10 nm. This distribution in size is generally undesirable, but the possibility of controlling the orientation(s) of particles can be very useful. The nano-scale range of sizes means that the particles exist as single magnetic domains, since the energy cost for forming domain walls is too high.

Table 1 Some nanoparticle systems formed by ion implantation methods

MAGNETIC SPECIES	HOST	REFERENCE
Ni	Al_2O_3	–
	SiO_2	–
Fe	YSZ [001], YSZ [110]	So2001
	Al_2O_3	–
	SiO_2	–
Co	Al_2O_3	Ho2000
$\text{Fe}_{1-x}\text{Pt}_x$	Al_2O_3	Wh2002a, Wh2003
	YSZ [001]; [110]; [111]	
	SiO_2	Va2002
$\text{Co}_{1-x}\text{Pt}_x$	Al_2O_3	Wi2003
	SiO_2	–

COMPETING ENERGY SCALES

In a ferromagnetic material, there are several energy scales that compete. This generality applies as well to the nanoparticle arrays investigated here. As illustrated in the adjoining figure for a collection of single domain particles, one can consider for a single particle its Zeeman energy that tends to align it with an external magnetic field; the randomizing effects of thermal energy $k_B T$; and the magneto-crystalline energy that tends to align the particle's magnetic moment with certain crystal directions, i.e., the crystallographic "easy axes." For the magnetic systems investigated in this work (Ni, Fe, Co, CoPt, and FePt), the magneto-crystalline anisotropy varies by about 3 orders of magnitude from the smallest (Ni) to the largest (FePt). This wide range leads to a range of importance, from negligible to dominant. Another competing energy term is the interaction between particles; magnetostatic effects are always present, while the possibility of exchange interactions between particles is negligible for well-separated particles in an insulating matrix. Next we consider several cases that illustrate dominant effects of these in some nanoparticle systems.

MAGNETIC RESPONSE of NANOPARTICLE ARRAYS

Ni in Al₂O₃

These materials were formed by implanting 750 keV Ni-ions into (0001) Al₂O₃ at room temperature. The host was misaligned slightly with the ion beam to avoid channeling effects, thereby providing a projected range of 320 nm with a spread in range of 70 nm. For doses of 5 and 20 × 10¹⁶ ions/cm², this corresponds to maximum concentrations in the matrix of ~2.5 and 10 %, respectively. Annealing

Zeeman Energy

$$\sim -m \cdot H$$

aligns magnetic moment m with applied field H

Magnetocrystalline Energy

$$\sim K_u V \sin^2 \theta + \dots$$

aligns magnetic moment m with preferred crystal directions

Thermal Energy

$$\sim k_B T$$

randomizes magnetic moments; makes spin waves; eventually destroys ferromagnetism.

Interaction Energy of particles

$$\sim \sum \sum m_i \cdot m_j / r_{ij}^3 + \dots$$

aligns magnetic moments with local, internal effective magnetic field

Fig. 1. A sketch of several competing energy scales in an array of single domain ferromagnetic nanoparticles. The upper two can be controlled in the laboratory via the applied magnetic field and temperature. The lower two can be affected by the choice of magnetic material and the concentration of nanoparticles.

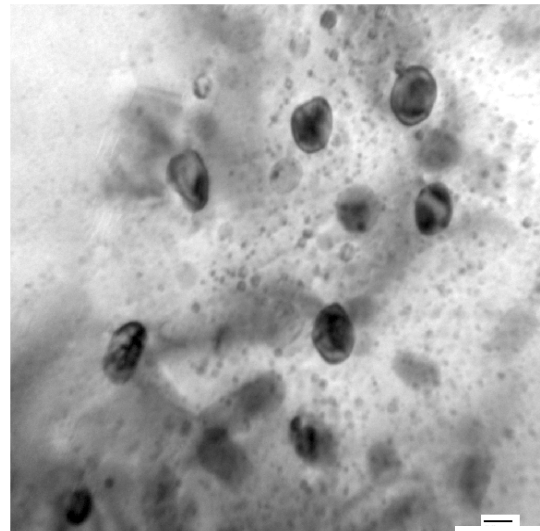


Fig. 2. A cross-sectional TEM image of Ni nanoparticles embedded in sapphire. Here the Ni-ion fluence was 1 × 10¹⁷ ions/cm².

for 2 hours in forming gas at 1100 °C led to the formation of roughly spherical particles, as shown in Fig. 2. A few particles have diameters near 20-30 nm, while most are quite small with diameters ~ 4 nm; all are well below the radius of ~ 43 nm for single domains in Ni. X-ray diffraction studies of these materials have shown that the Ni $\langle 111 \rangle$ axes align with the c -axis of the sapphire host, i.e. with the surface normal. For reference, bulk Ni metal has its magnetic easy axis along the $\langle 111 \rangle$ axes.

Magnetic studies on these and all other nanoparticle systems were conducted using a SQUID (Superconducting *Quantum Interference Device*) magnetometer. The instrument allows measurement of the bulk magnetic moment as a function of temperature for T in the range 5 – 400 K (and up to 800 K with a sample space heater). A superconductive magnet provides magnetic fields to ± 65 kOe = ± 6.5 T. The substrate (sapphire, SiO₂, etc.) generally contributes a substantial diamagnetic moment to the measured moment; in all cases shown, this background signal has been subtracted in order to obtain the ferromagnetic response of the nanoparticle systems.

Let us first consider the magnetic response of a dilute array of Ni particles, formed using a comparatively low fluence of 5×10^{16} ions/cm². The resulting magnetization M is shown as a function of magnetic field H in Fig. 3, for temperatures $T = 5$ and 300 K. The filled symbols

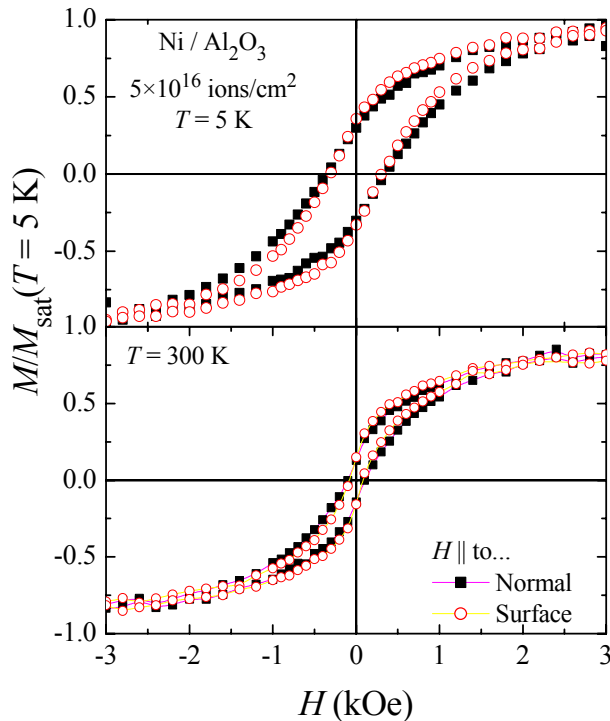


Fig. 3. The magnetization of an array of Ni-nanoparticles in sapphire [0001] at $T = 5$ and 300 K, with magnetic field applied normal to layer or parallel to it. Ion fluence 5×10^{16} ion/cm²

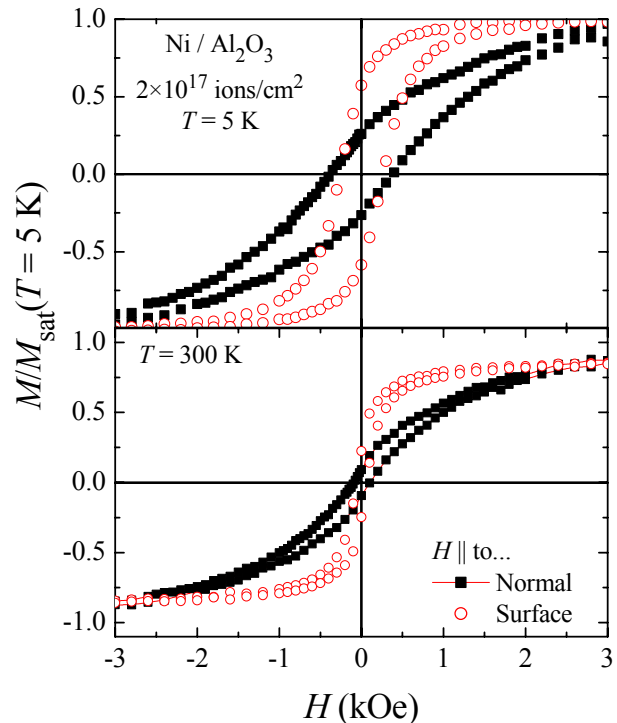


Fig. 4 As above, the magnetization of an array of Ni-nanoparticles in sapphire [0001] at $T = 5$ and 300 K, but with a 4 \times higher ion fluence and particle density.

show M for the case with field applied parallel to the surface normal, i.e., perpendicular to the buried layer; the open symbols show the case with H parallel to the surface, i.e., in-plane. In this relatively dilute system, the response is nearly isotropic, for both temperatures shown. The main effect of increased temperature is to decrease the width of the M - H loop and reduce the coercive field H_c . In relatively modest fields, the Zeeman energy dominates and the magnetization is easily saturated. At $T = 300$ K which is about $\frac{1}{2}$ of the Curie temperature T_c , the magnetization is reduced to $\sim 85\%$ of its value at low temperature, qualitatively demonstrating the thermal excitation of spin waves. Interactions between particles have little effect for this material.

In contrast, Fig. 4 shows the magnetization for a similarly prepared Ni-nanoparticle array with a 4-fold higher ion fluence. This produces a more dense layer, increasing the interparticle interactions. Qualitatively, the layer starts to resemble a thin (very discontinuous) film of soft ferromagnet, which is easily magnetized in its plane, but which is more difficult to magnetize out-of-plane. Indeed, that is precisely the behavior evident in Fig. 4: a shape-dominated easy axis in-plane, which minimizes the magnetostatic energy. Other magnetic features, including a blocked magnetization, temperature dependence of the magnetization, and remanence studies will be reported separately.

Fe in YSZ

These materials have been studied extensively, both experimentally [So2001] and in numerical simulations.[Sc2001], [Le2003] Compared with bulk metallic Ni where the ferromagnetic moment per atom is $0.61 \mu_B$ and the volume saturation magnetization $M_{\text{sat}} = 510$ G, bulk Fe has a moment of $2.22 \mu_B$ and $M_{\text{sat}} = 1740$ G. Magnetostatic interactions scale as M^2 , which is an order of magnitude larger in Fe than Ni. Consequently interaction effects are prominent, leading to M - H loops similar to those observed in Fig. 4. In addition, smaller in-plane anisotropies were observed for the particle system with preferred particle orientations. Numerical simulations have demonstrated that interaction effects dominate the magnetic response of these materials and stabilize the remanent magnetization to temperatures far above the blocking temperature for isolated particles (where the thermal energy ‘quickly’ randomizes the orientation of a single domain magnetic moment by exciting it over single particle energy barriers, e.g., from shape or magnetocrystalline anisotropy). Expressed differently, the interactions greatly inhibit the onset of superparamagnetism. It is clear that interaction effects are key to understanding the magnetic behavior of these Fe-based materials. [Sc2001], [Le2003]

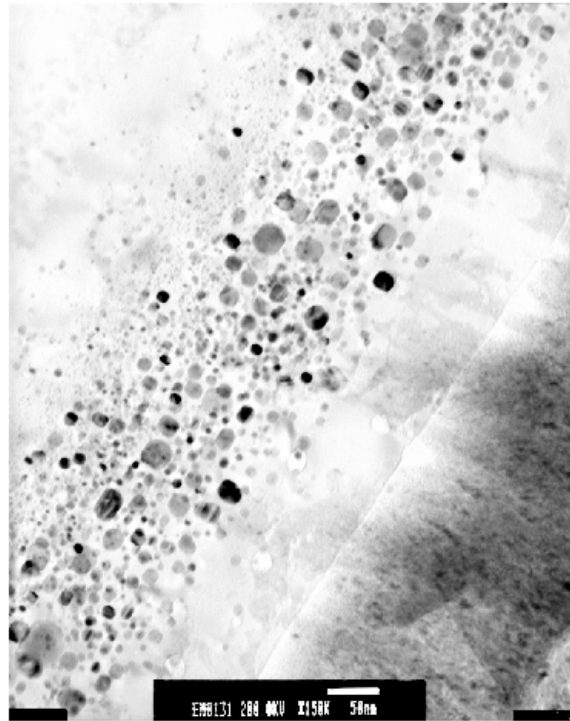


Fig. 5. A cross-sectional TEM image of $L1_0$ phase FePt nanoparticles, prepared by ion implantation into sapphire at elevated temperatures (550°C for Fe and 500°C for Pt). Annealing at 1100°C in Ar+4% H_2 formed relatively small particles (marker = 50 nm.)

$Fe_{1-x}Pt_x$ in Al_2O_3 and SiO_2

Interest in the FePt intermetallics was greatly stimulated by the report of Sun et al. [Su2000] on the formation of regular arrays of monodispersed FePt nanoparticles. With the block copolymer preparation used, the individual particles had randomly oriented crystallographic axes. In our studies, the materials were synthesized by sequential implantations of Fe followed by Pt ions. [Wh2002a], [Wh2002b], [Wh2003] For roughly equi-atomic stoichiometries x near 50 %, the FePt system can form an ordered intermetallic compound with the $L1_0$ structure. An example of resulting microstructure is shown in Fig. 5, where the implantations were conducted at elevated temperatures to lessen damage to the sapphire substrate; annealing was conducted in forming gas at 1100 °C. Close examination of Fig. 5 reveals faceting for many of the larger particles, associated with the preferred orientations discussed below. When implanted at lower temperatures, the substrate retains much more damage in the near surface layer, promoting the formation of more plate-like and extended structures.[Wh2003] In addition, the influence of annealing or post-annealing in vacuum and/or oxidizing atmospheres has been investigated. [Wh2004] With other preparation methods, differing morphologies such as nanowires [Zh2003] can be formed.

These materials are quite interesting, as the magnetocrystalline anisotropy in the ordered $L1_0$ phase can be very high. [We2000] In the present case, X-ray diffraction studies of materials with $x \sim 50$ % show the presence of superlattice reflections that are forbidden in the disordered alloy, and the intensity of these reflections indicates that the nanoparticles are fully ordered and likely contain Al from the matrix. The particles are oriented primarily with the $\langle 111 \rangle$ and $\langle 110 \rangle$ axes

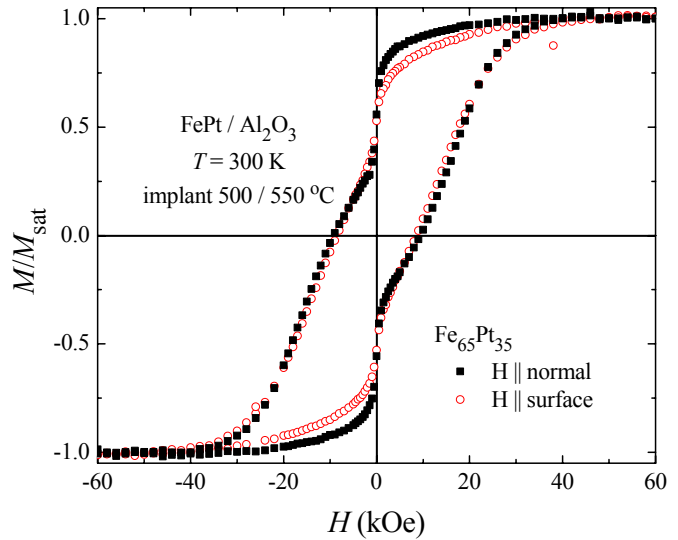


Fig. 6. The normalized magnetization of $Fe_{65}Pt_{35}$ nanoparticles, plotted vs. magnetic field H applied either out-of-plane or in-plane. Note the large coercive field $H_c = 10$ kOe.

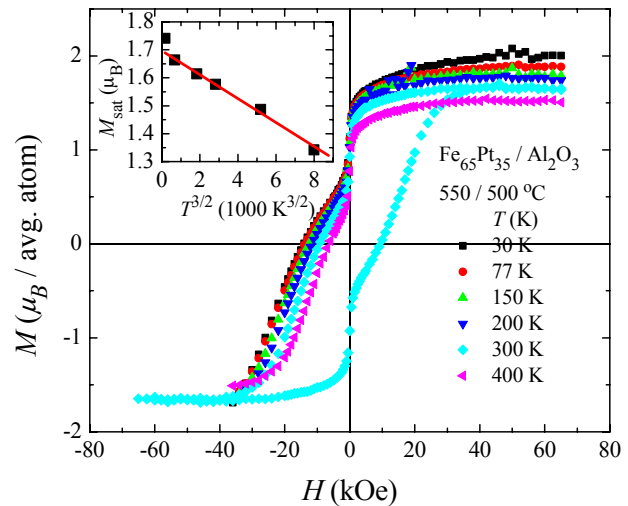


Fig. 7. The magnetization of $Fe_{65}Pt_{35}$ nanoparticles at the temperatures shown, plotted versus magnetic field H applied \perp surface. The inset shows the saturation magnetization M_{sat} as a function of $T^{3/2}$ as appropriate for spin waves in 3D.

of the face centered tetragonal lattice oriented along the normal to the surface.

The magnetic response $M(H)$ of a chemically ordered nanoparticle alloy with composition $\text{Fe}_{65}\text{Pt}_{35}$ is shown in Fig. 6. Even with the sample temperature of 300 K for these data, the coercivity is quite high with $H_c = 10$ kOe. This is due to the large magnetocrystalline anisotropy, which dominates the behavior of these small, single domain particles. It is also evident in Fig. 6 that the in-plane and out-of-plane responses are very similar, showing that any effects of interactions are masked by much larger single particle anisotropy effects. Since Fig. 5 shows the particles to be nearly equiaxed, single particle shape anisotropy can be neglected, and one concludes that magnetocrystalline anisotropy dominates in this case. In regard to the large magnetic hysteresis and high values of the coercive field, let us note that the $L1_0$ phase field exists over a considerable compositional range of Pt contents $x \approx 35 - 55$ at %, which allows some “tuning” of the magnetic properties. We observe the highest coercivities $H_c = 20 - 25$ kOe for $x \sim 45$ at. %.

As the temperature increases, thermal effects compete with the microscopic ferromagnetic interaction between spins, leading to the excitation of magnons. For $T \ll T_c$, the Curie temperature, this leads to the formation of spin waves in bulk materials. The spin wave dispersion in 3D has a characteristic temperature dependence for the spontaneous magnetization, $[1 - \xi T^{3/2}]$. To test this scenario, we plot the saturation magnetization M_{sat} vs. $T^{3/2}$ in the inset to Fig. 7. The resulting linearity shows that the spin wave dependence describes reasonably well the excitations in this $\text{Fe}_{65}\text{Pt}_{35}$ nanoparticle system. Interestingly, the $T^{3/2}$ dependence persists to surprisingly high temperatures, at least 400 K in the data shown in the inset. Since the present composition has $T_c \approx 700$ K, this corresponds to ~ 60 % of the fractional temperature range, well beyond the expected limits of validity for spin waves in bulk ferromagnets. Another interesting feature is the magnitude of the spin wave coefficient $\xi = 2.8 \times 10^{-5} \text{ K}^{-3/2}$. To put this into context, note that bulk Ni (with a similar $T_c = 627$ K) has $\xi = 0.75 \times 10^{-5} \text{ K}^{-3/2}$, i.e., smaller by a factor of ~ 4 . We have observed a similar difference when comparing Fe nanoparticles with bulk Fe. For both the Fe and FePt particles, it is much easier to excite spin waves with the associated reduction in magnetization in nanoparticle systems, compared with bulk materials. Qualitatively this may be attributed to a reduced spin wave stiffness arising from the near proximity of the surface for many spins, especially in the numerous small particles.

Finally, let us consider the high temperature limit. As an example, Fig. 8 shows the temperature dependence of

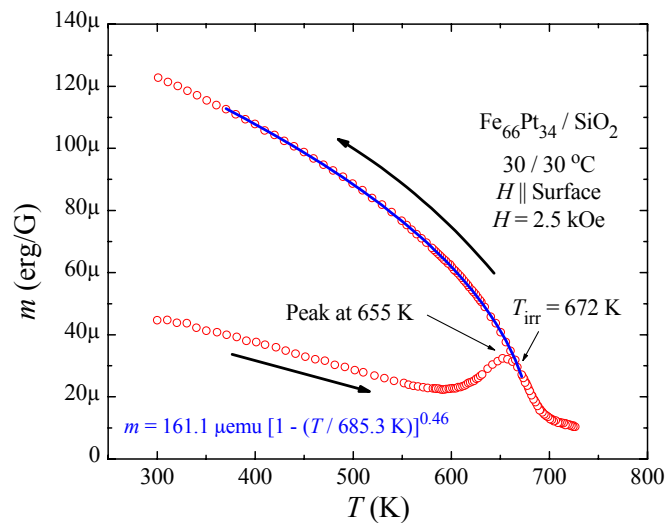


Fig. 8. The magnetization of $\text{Fe}_{66}\text{Pt}_{34}$ nanoparticles in SiO_2 , implanted at room temperature. A field of 2.5 kOe was applied in-plane after cooling in zero field. After warming above the Curie temperature, the sample was cooled in the same 2.5 kOe field.

the magnetic moment of L1₀ phase Fe₆₆Pt₃₄ particles in amorphous SiO₂. Like the FePt/Al₂O₃ materials discussed above, the samples are highly hysteretic and have large coercivity at lower temperatures. For the present study, the sample was first demagnetized and then a magnetic field of 2.5 kOe was applied at 300 K. As the temperature was increased, the resulting magnetic moment m decreased slowly, then passed through a peak at 653 K. The Curie temperature is $T_c = 683$ K; the finite signal at still higher temperature is an induced moment in the paramagnetic state due to the applied field. Cooling in the same 2.5 kOe field at first retraced the curve of $m(T)$, and then the warming and cooling curves separated at an irreversibility temperature $T_{irr} = 672$ K.

In terms of competing energy scales, we interpret the peak as follows: on its low side, m rises due to a decreasing magnetocrystalline anisotropy, which finally allows the particles to align with the external field, i.e., the Zeeman energy becomes dominant over the magnetocrystalline energy. This occurs very near the Curie point, however, so further increases in T rapidly diminish the spontaneous (and experimentally observed) magnetization. This qualitative interpretation is consistent with the thermal reversibility of m for $T > T_{irr}$. At the Curie point, of course, thermal disorder overwhelms all other magnetic energy scales and the ferromagnetism gives way to paramagnetism with no spontaneous moment. As shown by the solid line in Fig. 8, the field-cooling data can be described by a “critical point” relation with an exponent near $\frac{1}{2}$ in this case. Further details will be published elsewhere.

CONCLUSIONS

This survey has considered the formation of magnetic nanoparticle systems formed using ion implantation and thermal annealing methods. As noted, this approach allows for the formation of encapsulated nanoparticles with substantial control over their composition. Furthermore, crystalline hosts often impart the particles with preferred orientations and faceting. Magnetic studies of the resulting materials reveal a competition among multiple energy scales, with thermal and Zeeman energies continuously controllable. One can control interparticle interactions (to some extent) by choosing the concentration of particles. Finally, the magnetocrystalline anisotropy can be varied widely by choosing the magnetic species, ranging from low (e.g., Ni) to quite high (e.g., FePt at various compositions). Overall, the materials provide a well-characterized set of materials for testing and exploring the competition of magnetic energies at the nanoscale.

The Oak Ridge National Laboratory is managed by UT-Battelle, LLC for the United States Department of Energy under contract No. DE-AC05-00OR22725.

REFERENCES

- [Bi1994] I. M. L. Billas, A. Châtelain, and W. A. de Heer, "Magnetism from the Atom to the Bulk in Iron, Cobalt, and Nickel Clusters," *Science* **265**, 1682 (1994).
- [Ha1998] M. F. Hansen and S. Mørup, "Models for the dynamics of interacting magnetic nanoparticles," *J. Magn. Magn. Mater.* **184**, L262 (1998).
- [Ha2001] J. W. Harrell, S. Wang, D. E. Nikles, and M. Chen, "Thermal effects in self-assembled FePt nanoparticles with partial chemical ordering," *Appl. Phys. Lett.* **79**, 4393 (2001).
- [Ho2000] S. Honda, F. A. Modine, T. E. Haynes, A. Meldrum, J. D. Budai, K. J. Song, J. R. Thompson, and L. A. Boatner, "The Formation of High-Coercivity, Oriented, Nanophase Cobalt Precipitates in Al₂O₃ Single Crystals by Ion Implantation," p. 71–76 in *Nanophase and Nanocomposite Materials III*, eds. S. Komarneni, J. C. Parker, and H. Haun, *Mat. Res. Soc. Symp. Proc.* Vol. **581** (Materials Research Society, Pittsburgh, 2000).
- [Ko1999] R. H. Kodama, "Magnetic nanoparticles," *J. Magn. Magn. Mater.* **200**, 359 (1999).
- [Le2003] H. K. Lee, T. C. Schulthess, G. Brown, D. P. Landau, K. D. Sorge, and J. R. Thompson, "Magnetic Properties of Fe Nanocubes with Magnetostatic Interactions," *J. Appl. Phys.* **93**, (10) 7047 (2003).
- [Le1996] D. L. Leslie-Pelecky and R. D. Rieke, "Magnetic properties of nanostructured materials," *Chem. Mater.* **8**, 1770 (1996).
- [Pi1985] S. T. Picraux and P. S. Peercy, "Ion Implantation of Surfaces," *Sci. Am.* **252**, 102 (1985).
- [Sc2001] T. C. Schulthess, M. Benakli, P. B. Visscher, K. D. Sorge, J. R. Thompson, F. A. Modine, T. E. Haynes, L. A. Boatner, G. M. Stocks, and W. H. Butler, "Role of Magnetostatic Interactions in Assemblies of Fe Nanoparticles," *J. Appl. Phys.* **89**, 7594 (2001).
- [Sk2003] R. Skomski, "Nanomagnetics," *J. Phys.: Condens. Matter* **15**, R841 (2003).
- [So2001] K. D. Sorge, J. R. Thompson, T. C. Schulthess, F. A. Modine, T. E. Haynes, Shin-ichi Honda, A. Meldrum, J. D. Budai, C. W. White, and L. A. Boatner, "Oriented, Single Domain Fe Nanoparticle Layers in Single Crystal Yttria-Stabilized Zirconia," *IEEE Trans. Magn.* **37**, (4) 2197 (2001).
- [Su2000] S. Sun, C. B. Murray, D. Weller, L. Folks, and A. Moser, "Monodisperse FePt nanoparticles and ferromagnetic FePt nanocrystal superlattices," *Science* **287**, 1989 (2000).
- [Va2002] C. E. Vallet, C. W. White, S. P. Withrow, J. D. Budai, L. A. Boatner, K. D. Sorge, J. R. Thompson, K. S. Beaty, and A. Meldrum, "Magnetic Force Microscopy of

Ferromagnetic Nanoparticles Formed in Al_2O_3 and SiO_2 by Ion Implantation,” *J. Appl. Phys.* **92**, 6200–04 (2002).

[We1999] D. Weller and A. Moser, “Thermal Effect Limits in Ultrahigh-Density Magnetic Recording,” *IEEE Trans. Magn.* **35**, 4423 (1999).

[We2000] D. Weller, A. Moser, L. Folks, M. E. Best, W. Lee, M. F. Toney, M. Schwickert, J.-U. Thiele, and M. F. Doerner, “High K_u Materials Approach to 100 Gbit/in²,” *IEEE Trans. Magn.* **36**, 10 (2000).

[Wh2002a] C. W. White, S. P. Withrow, J. D. Budai, L. A. Boatner, K. D. Sorge, J. R. Thompson, K. S. Beaty, and A. Meldrum, “Ferromagnetic FePt Nanoparticles Formed in Al_2O_3 by Ion Implantation,” *Nucl. Instrum. Methods Phys. Res. B* **191**, 437 (2002).

[Wh2002b] C. W. White, S. P. Withrow, J. D. Budai, L. A. Boatner, K. D. Sorge, J. R. Thompson, K. S. Beaty, and A. Meldrum, “Formation of Ferromagnetic FePt Nanoparticles by Ion Implantation,” p. W7.7.1 in *Nanoparticulate Materials*, Vol. **704** eds. R. K. Singh, R. Partch, M. Muhammed, M. Senna, and H. Hofmann (Materials Research Society, Warrendale, Pennsylvania, 2002).

[Wh2003] C. W. White, S. P. Withrow, K. D. Sorge, A. Meldrum, J. D. Budai, J. R. Thompson, and L. A. Boatner, “Oriented Ferromagnetic Fe-Pt Alloy Nanoparticles Produced in Al_2O_3 by Ion-Beam Synthesis,” *J. Appl. Phys.* **93**, 5656 (2003).

[Wh2004] C. W. White, S. P. Withrow, J. M. Williams, J. D. Budai, A. Meldrum, K. D. Sorge, J. R. Thompson, and L. A. Boatner, “Fe-Pt Nanoparticles Formed in Al_2O_3 by Ion-Beam Synthesis: Annealing Environment Effects,” (submitted for publication, 2004).

[Wi2003] S. P. Withrow, C. W. White, J. D. Budai, L. A. Boatner, K. D. Sorge, J. R. Thompson, and R. Kalyanaraman, “Ion Beam Synthesis of Magnetic Co-Pt Alloys in Al_2O_3 ,” *J. Magn. Mater.* **260**, 319 (2003).

[Xu2003] Y. Xu, Z. G. Sun, Y. Qiang, and D. J. Sellmyer, “Magnetic properties of L_{10} FePt and FePt:Ag nanocluster films,” *J. Appl. Phys.* **93**, 8289 (2003).

[Zh2003] Z. Zhang, D. A. Blom, Z. Gai, J. R. Thompson, J. Shen, and S. Dai, “High-Yield Solvothermal Formation of Magnetic CoPt Alloy Nanowires,” *J. Am. Chem. Soc.* **125**, 7528 (2003).